Journal of Alloys and Compounds 509 (2011) 3537–3540

Contents lists available at ScienceDirect

Journal of Alloys and Compounds

journal homepage: www.elsevier.com/locate/jallcom

The effects of $Bi(Mg_{2/3}Nb_{1/3})O_3$ on piezoelectric and ferroelectric properties of $K_{0.5}Na_{0.5}NbO_3$ lead-free piezoelectric ceramics

Jingbo Zhao [a,b,*], Hongliang Du [a,b], Shaobo Qu [a], Jiafu Wang [a], Hongmei Zhang [a], Yiming Yang [a], Zhuo Xu [c]

[a] *College of Science, Air Force Engineering University, Xi'an 710051, Shaanxi, China*
[b] *State Key Laboratory of Solidification Processing, Northwestern Polytechnical University, Xi'an 710072, China*
[c] *Electronic Materials Research Laboratory, Key Laboratory of Educational Ministry, Xi'an Jiaotong University, Xi'an 710049, China*

ARTICLE INFO

Article history:
Received 5 May 2010
Received in revised form 20 July 2010
Accepted 22 July 2010
Available online 30 July 2010

Keywords:
Lead-free ceramics
Piezoelectric
Composition fluctuation
Diffusion
Temperature stability

ABSTRACT

To improve the temperature stability of piezoelectric properties of $Na_{0.5}K_{0.5}NbO_3$ (KNN)-based ceramics, $Bi(Mg_{2/3}Nb_{1/3})O_3$ (BMN) was used to modify $Na_{0.5}K_{0.5}NbO_3$ (KNN)-based ceramics by a conventional sintering technique. Piezoelectric and ferroelectric properties of $0.99K_{0.5}Na_{0.5}NbO_3$–$0.01Bi(Mg_{2/3}Nb_{1/3})O_3$ ceramics were studied. It is found that 0.01BMN–0.99KNN ceramics exhibits stable piezoelectric properties as the temperature changes due to the composition fluctuation on B sites ($d_{33} \approx 130$ pC/N, dielectric loss $\mathrm{tg}\,\theta \leq 5\%$ in the range 25–300 °C). These results indicate that these materials are promising lead-free piezoelectric ceramic candidates for practical applications.

1. Introduction

Conventional piezoelectric ceramics or single crystals are mostly Pb-based perovskite materials, in which lead oxides take up at least 70 wt% [1]. As is well known, lead usually brings about great threat to the environment. In recent years, some countries have required all new electronic products to be lead-free for the sake of protecting the environment and human health. Therefore, it is urgent to develop lead-free piezoelectric materials. In the last few years, $(K_{0.5}Na_{0.5})NbO_3$ (KNN)-based lead-free materials exhibit piezoelectric properties which have been demonstrated to be comparable to conventional $Pb(Zr,Ti)O_3$ ceramics [2–12]. The enhanced dielectric and piezoelectric properties in these systems had initially been attributed to the effects of the MPB separating the orthorhombic and tetragonal phases. It was later found that the enhanced properties were in fact caused by the PPT (polymorphic phase transition) [13–16].

However, this transition correspondingly results in a strong temperature dependence, which has become gradually one of the key problems currently. Zhang et al. [17] prepared $CaTiO_3$-modified KNN–$LiSbO_3$ materials with greatly improved temperature stability ($d_{15} \approx 260$ pC/N in the range −50 to 200 °C). Wu et al. [18,19] also prepared KNN ceramics with improved temperature stability ($d_{33} \approx 250$ pC/N in the range 10–70 °C) and their main idea was to improve the temperature stability of KNN ceramics by shifting the PPT below room temperature. This method also results in a decrease of the Curie point. However, the temperatures are not high enough for these materials to be used at high temperature applications such as automotive, aerospace, and other related industrial applications. Therefore, it is necessary to develop lead-free piezoelectric ceramics for high temperature applications.

To further improve the temperature stability of KNN ceramics for high temperature applications, the diffusion phase transition characteristics in relaxor ferroelectrics are introduced into KNN ceramics. It is well known that relaxor ferroelectrics are commonly thought to be complex perovskite with ABO_3 type cell unit and are characterized by the ionic disorder resulting from the random occupation of the B site position by at least two different valence cations [20–22]. The typical relaxor ferroelectrics PMN ($Pb(Mg_{1/3}Nb_{2/3})O_3$) is known for its good properties. Meanwhile, the chemistry of Pb is known to be very important to the properties of Pb-based piezoelectric alloys because most of the relevant piezoelectric alloys have only Pb on the A site of their perovskite structure. Cohen [23] confirmed that the hybridization between Pb 6p and O 2p orbitals is responsible for large piezoelectric responses in Pb-based piezoelectric materials. Bi^{3+} is isoelectronic with Pb^{2+} and shows a valence electron configuration of 6s26p0. Based on the above-mentioned considerations, we try to introduce the Bi^{3+} to A site, and Mg^{2+} to B site in KNN

---

[*] Corresponding author at: College of Science, Airforce Engineering University, Xi'an 710051, Shaanxi, China. Tel.: +86 29 8250 4542; fax: +86 29 8530 7774.
E-mail address: chjzjb@163.com (J. Zhao).

0925-8388/$ – see front matter © 2010 Elsevier B.V. All rights reserved.
doi:10.1016/j.jallcom.2010.07.153

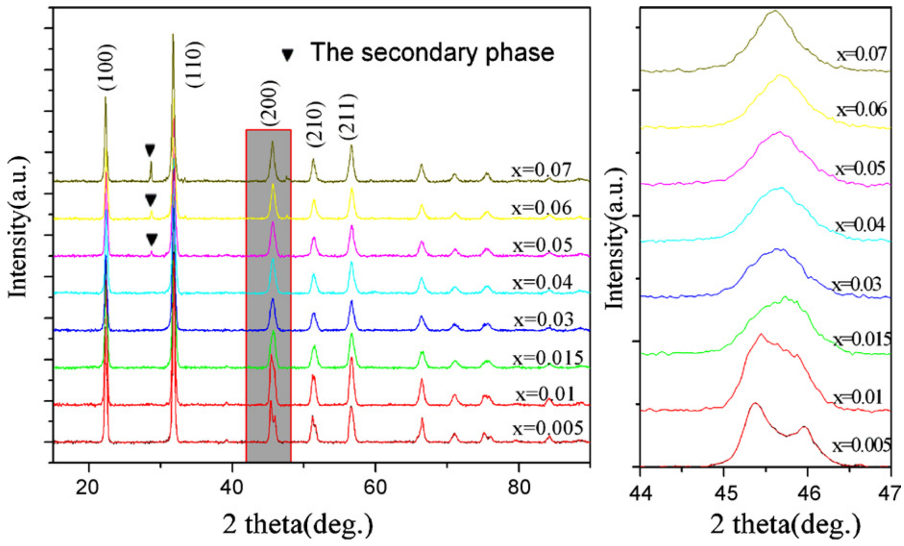

Fig. 1. X-ray powder diffraction pattern of $(1-x)$KNN–xBMN ceramics at room temperature (25 °C).

ceramics; thus, $Bi(Mg_{2/3}Nb_{1/3})O_3$ is used to develop KNN ceramics.

In this paper, we prepared $Bi(Mg_{2/3}Nb_{1/3})O_3$-modified $Na_{0.5}K_{0.5}NbO_3$ (KNN), i.e., $(1-x)Na_{0.5}K_{0.5}NbO_3$ (KNN)–$xBi(Mg_{2/3}Nb_{1/3})O_3$ [$(1-x)$KNN–xBMN] lead-free piezoelectric ceramics, by the conventional solid-state sintering method. The addition of BMN leads to a polymorphic phase transition between ferroelectric orthorhombic and rhombohedral phases ($x=0.01$), resulting in high electrical properties and improved temperature stability from 20 to 300 °C and lower dielectric loss ($\leq 5\%$).

2. Experimental procedure

$xBi(Mg_{2/3}Nb_{1/3})O_3-(1-x)(K_{0.5}Na_{0.5})NbO_3$ (xBMN–$(1-x)$KNN) ($x=0.005$, 0.01, 0.015, 0.03, 0.04, 0.05, 0.06 and 0.07) ceramics were prepared using the conventional solid-state sintering method. Reagent-grade oxide and carbonate powders of K_2CO_3 (99.0%), Na_2CO_3 (99.8%), Bi_2O_3 (99.0%), Nb_2O_5 (99.9%), and MgO (98%) were used as the starting materials. Before weighed, these powders were separately dried in an oven at 120 °C for 5 h, milled for 24 h using a planetary milling with zirconia ball media and ethanol, calcined at 900 °C for 5 h. Then, these powders were ball-milled again for 12 h, dried, and pressed into disks with diameters of 12 mm and thickness of 1 mm under 300 MPa using 5 wt% polyvinyl alcohol (PVA) as the binder. After the PVA was burned off, the pellets were sintered at 1140–1160 °C for 2 h in the sealed Al_2O_3 crucibles (1140 °C for 2 h when $x \geq 0.01$; 1160 °C for 2 h when $x=0.005$). The obtained samples were polished. Silver paste was fired on both sides of the samples at 810 °C for 20 min as the electrodes for the sake of measurements.

The microstructure evolution was observed using a scanning electron microscopy (SEM) (model JSM-6360, JEOL, Tokyo, Japan). The dielectric spectrum measurements were performed using the LCR meter (TH2816, Tonghui Electronics, Chang Zhou, China) with a heat rate of 2 °C/min in a temperature range of 25–500 °C and a frequency range of 1–100 kHz. The samples were painted with silver pastes and poled in silicone oil at 3 kV/mm for 15 min at 80 °C. The piezoelectric constant was measured using a piezoelectric d_{33}-meter (ZJ-3A). The polarization versus electric (P–E) hysteresis loop was observed using the TF2000 test equipment. TPP% (temper-

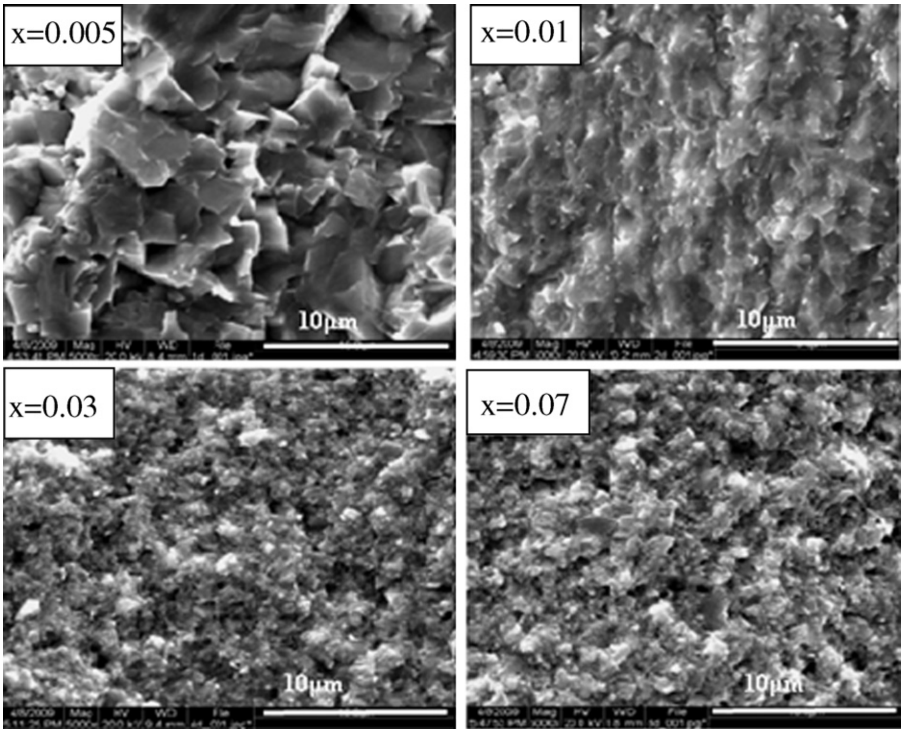

Fig. 2. The SEM micrograph of fracture surface of KNN–xBMN ($x=0.005$, 0.01, 0.03, and 0.07) ceramics.

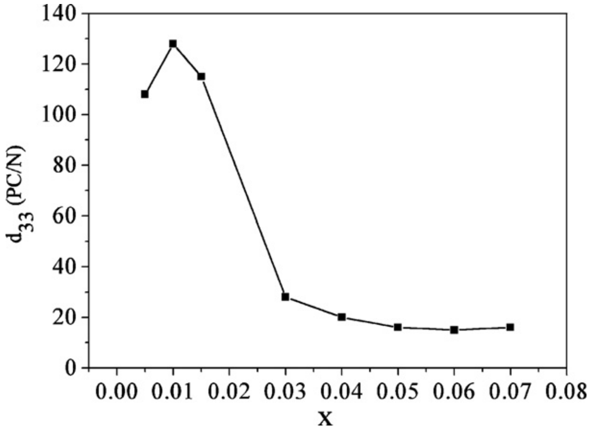

Fig. 3. The piezoelectric properties of $(1-x)$KNN–xBMN ceramics as the function of composition.

ature properties of piezoelectric) is used to describe the piezoelectric temperature properties, and it is calculated according to the following formula:

$$\mathrm{TPP\%} = \frac{(d_{33,\max} - d_{33,\min})}{d_{33,\max}} \times 100\%$$

where $d_{33,\max}$ and $d_{33,\min}$ are, respectively, the maximal piezoelectric constant and the minimal piezoelectric constant in a given temperature range.

3. Results and discussion

Fig. 1 shows the XRD patterns of $(1-x)$KNN–xBMN ($x = 0.005$, 0.01, 0.015, 0.03, 0.04, 0.05, 0.06, and 0.07) ceramics at room temperature. This material shows a changing symmetry with increasing BMN content; when $x = 0.005$, the material displays a typical orthorhombic symmetry at room temperature. However, the structure changes rapidly with the addition of BMN. When $0.03 \geq x > 0.01$, it becomes a rhombohedral structure; as reported in foregoing research [24]; the transitional point for the structure change can be identified to be near $x = 0.01$; with further increasing BMN content, it becomes cubic when $x = 0.04$; the secondary phase has been found with $x \geq 0.05$, and the secondary phase is pyrochlore phase.

Fig. 2 shows the SEM micrograph of fracture surface of KNN–xBMN ($x = 0.005$, 0.01, 0.03, and 0.07) ceramics sintered at 1140 °C for 2 h. It can be seen that the KNN–0.005BMN ceramics is dense, and the grain size is 2–5 μm; the grain size decreases rapidly with increased BMN content; when $x \leq 0.01$, the grain is below 1 μm, but the fracture surface for the case with $x = 0.01$ is very dense, without any poles and impurity in the micrograph. It is well known that the grain size and density benefit to the piezoelectric properties. As a result, although the KNN–0.01BMN ceramics is very dense, the piezoelectric constant ($d_{33} = 128$ pC/N) is not high because of small grain size.

Fig. 3 shows the piezoelectric properties of $(1-x)$KNN–xBMN ceramics with different compositions. It is evident that the properties exhibit a strong compositional dependence. As expected, the best electrical properties of the polarized solid solutions are present in the materials with $x = 0.01$. The piezoelectric constant $d_{33} = 128$ pC/N, then decay very rapidly, regardless of the subsequent decrease in grain size with further addition of BMN. The reason that the piezoelectric properties can not be improved notably lies in that there is a lack of abrupt phase transition near room temperature with increased BMN content because of the diffusion characteristics resulting from composition fluctuation on B sites. Meantime, the pyrochlore phase deteriorated the piezoelectric properties when $x \geq 0.05$ (Fig. 1).

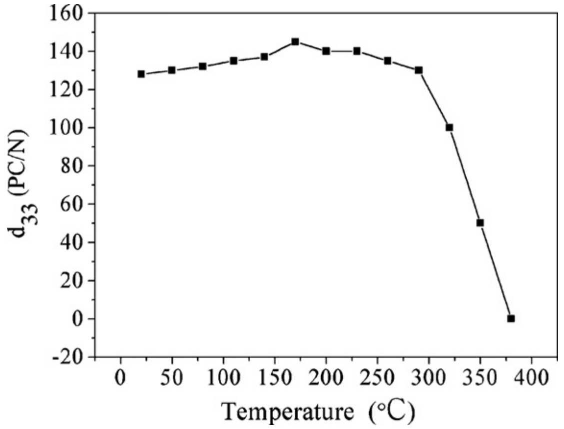

Fig. 4. The piezoelectric properties of $(1-x)$KNN–xBMN ceramics as the function of temperature.

Fig. 4 gives the piezoelectric properties of 0.99KNN–0.01BMN ceramics as the function of temperature. It is evident that the temperature stability of piezoelectric constant is good (TPP% = 16%, $d_{33} \approx 130$ pC/N in the range 20–300 °C). In our opinions, the improved temperature stability of piezoelectric constant was caused by the diffusion phase transition. It is well known that there is a PPT at about 200 °C in pure KNN. In this paper, we introduce the composition fluctuation on B site (Nb^{5+} and Mg^{2+}), which results in the diffusion phase transition near PPT. As expected, the temperature stability of piezoelectric properties is improved.

Fig. 5 shows dielectric permittivity of KNN–0.01BMN ceramics as the function of temperature and frequency; the T_c and T_{o-t} as function of composition at 100 kHz has also been shown in the same figure. It can be seen that KNN–0.01BMN ceramics have obvious diffusion phase transition characteristics, and the diffusion degree increases with frequency. Meantime, it can also be seen that the temperature range of PPT is widened and becomes a wide phase transition range. For the relaxor ferroelectrics, the reciprocity of the dielectric constant and temperature follows the Uchino and Nomura function, a modified Curie–Weiss law [25],

$$\frac{1}{\varepsilon} - \frac{1}{\varepsilon_m} = \frac{(T - T_m)^{\gamma}}{C}$$

where C is the Curie constant and γ is a diffusion coefficient ranging from one (a normal ferroelectric) to two (an ideal relaxor ferroelectric). In order to confirm the diffuse phase transition behavior of KNN–0.01BMN ceramics, the plots of $\log(1/\varepsilon - 1/\varepsilon_m)$ as the function of $\log(T - T_m)$ at 10 kHz are given in Fig. 6. The slope of fitting

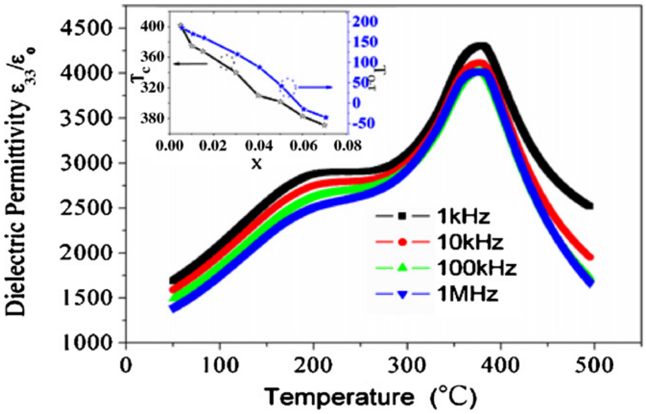

Fig. 5. Dielectric permittivity of KNN–0.01BMN ceramics as the function of temperature and frequency.

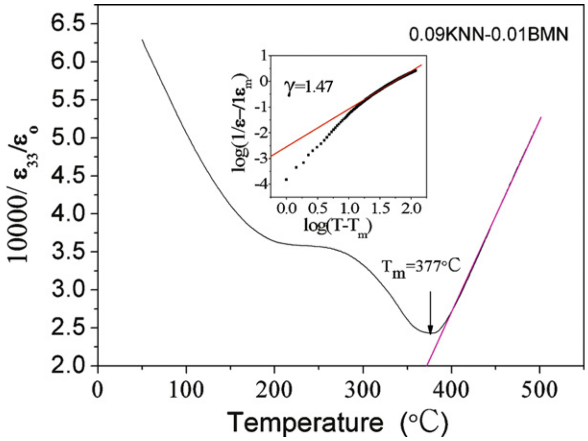

Fig. 6. The plots of $\log(1/\varepsilon - 1/\varepsilon_m)$ as a function of $\log(T - T_m)$ at 10 kHz for KNN–0.01BMN ceramics.

curves is used to determine the γ value. It can be calculated that $\gamma = 1.47$. The relaxor behavior can be explained by the composition fluctuation theory, the superparaelectricity theory, the merging of micropolar into macropolar regions, and random-field mode [20,26–29]. In this solid solution of KNN–0.01BMN, K^+ (0.164 nm, CN = 12), Na^+ (0.139 nm, CN = 12) and Bi^{3+} (0.13 nm, CN = 12) occupy the A sites of ABO_3 perovskite structure because of their large ionic radius, while Nb^{5+} (0.064 nm, CN = 6), Mg^{2+} (0.072 nm, CN = 6) ions occupy the B sites. Therefore, the local order–disorder of the crystal structure gives rise to polar clusters of nanometric size or polar nanoregions (PNRs), which are embedded in the disordered matrix. The dielectric properties of relaxors are believed to be resulted from the complex response of all the PNRs and matrix [30].

Fig. 7 shows the dielectric loss of $(1-x)$KNN–xBMN ($x = 0.005$–0.07) ceramics sintered at 1140–1160 °C for 2 h. It can be seen that the dielectric loss is below 5% in the range 20–300 °C for $x = 0.01$, which demonstrates that KNN–0.01BMN ceramics has important engineering application values. The low loss of KNN–0.01BMN ceramics should be mainly attributed to high density of KNN–0.01BMN ceramics, as can be seen in Fig. 2. Fig. 8 shows typical P–E hysteresis loops (at 1 Hz) of KNN–BMN ceramics measured at room temperature. When $x = 0.005$–0.015, the remnant polarization Pr is ~24 $\mu C/cm^2$ with the BMN modification; when $x \geq 0.03$, the remnant polarization Pr is decreased to 5 $\mu C/cm^2$. From Fig. 1, we can find the phase change from rhombohedral structure to cubic structure when $x \geq 0.03$, and the symmetry decreased rapidly, which caused that the remnant polarization decreases rapidly and large numbers of micro-domains occur.

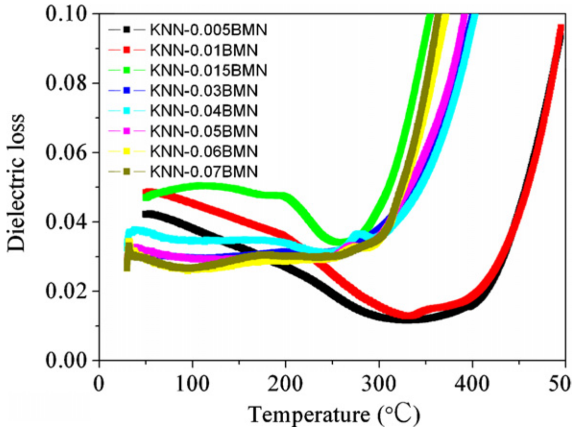

Fig. 7. The dielectric loss of $(1-x)$KNN–xBMN ($x = 0.005$–0.07) ceramics sintered at 1140 °C for 2 h.

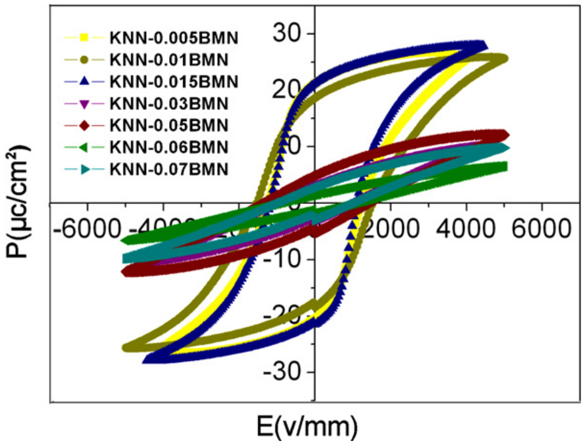

Fig. 8. P–E hysteresis loops (at 1 Hz) of KNN–BMN ceramics measured at room temperature.

4. Conclusions

a. The $(1-x)$KNN–xBMN ($x = 0.01$) ceramics show improved temperature stability ($d_{33} \approx 130$ pC/N, $\mathrm{tg}\,\theta \leq 5\%$ in the range 20–300 °C). The improved temperature stability of piezoelectric constant is probably caused by the diffusion phase transition.
b. Though d_{33} value of BMN-modified KNN ceramics is not very high, the stability is improved up to 300 °C, which is important for application at high temperature.
c. The introduction of diffusion mechanism into KNN ceramics improves the temperature stability of piezoelectric properties, which is useful in other materials systems.

Acknowledgements

This work was supported by National Natural Science Foundation of China (Nos. 10804130 and 60871027), Shaanxi Provincial Natural Science Foundation (No. 2009JQ1001), and Key Laboratory of Electrical Insulation and Power Equipment (EIPE10202).

References

[1] B. Jaffe, W.R. Cook, H. Jaffe, Piezoelectric Ceramics, Academic Press, NY, 1971.
[2] Y. Saito, H. Takao, T. Tani, Nature 432 (2004) 84–87.
[3] X. Li, J. Zhu, M. Wang, J. Alloys Compd. 499 (2010) L1–L4.
[4] J.G. Wu, D.X. Xiao, Y.Y. Wang, J. Alloys Compd. 476 (2009) 782–786.
[5] Q.Y. Yin, S. Yuan, Q. Dong, C. Tian, J. Alloys Compd. 491 (2010) 340–343.
[6] E. Li, R. Suzuki, T. Hoshina, Appl. Phys. Lett. 94 (2009) 132903.
[7] S.J. Zhang, R. Xia, T.R. Shrout, J. Appl. Phys. 100 (2006) 104108.
[8] B. Zhang, J. Li, K. Wang, J. Am. Ceram. Soc. 89 (2006) 1605.
[9] Q. Zhang, B.-P. Zhang, H.-T. Li, P.-P. Shang, J. Alloys Compd. 490 (2010) 260–263.
[10] Y. Chang, Z. Yang, L. Wei, J. Am. Ceram. Soc. 90 (2007) 1656–1658.
[11] L. Su, K. Zhu, L. Bai, J. Qiu, H. Ji, J. Alloys Compd. 493 (2010) 186–191.
[12] C. Lei, Z.G. Ye, Appl. Phys. Lett. 93 (2008) 042901.
[13] G.Z. Zang, J.F. Wang, H.C. Chen, Appl. Phys. Lett. 88 (2006) 212908.
[14] S.J. Zhang, R. Xia, T.R. Shrout, J. Electroceram. 19 (2007) 251.
[15] Y. Dai, X. Zhang, G. Zhou, Appl. Phys. Lett. 90 (2007) 262903.
[16] E.K. Akdogan, K. Kerman, M. Abazari, Appl. Phys. Lett. 92 (2008) 112908.
[17] S.J. Zhang, R. Xia, T.R. Shrout, Appl. Phys. Lett. 91 (2007) 132913.
[18] J.G. Wu, D.Q. Xiao, Y.Y. Wang, Scripta Mater. 59 (2008) 750–752.
[19] J.G. Wu, D.Q. Xiao, Y.Y. Wang, J. Appl. Phys. 104 (2008) 024102.
[20] L.E. Cross, Ferroelectrics 76 (1987) 241.
[21] D. Viehland, M. Wutting, L.E. Cross, Ferroelectrics 123 (1991) 71.
[22] V. Westphal, W. Kleemann, M.D. Glinchuk, Phys. Rev. Lett. 68 (1992) 847.
[23] R.E. Cohen, Nature 358 (1992) 136.
[24] J. Zhao, S. Qu, H. Du, Z. Xu, Ferroelectrics 404 (2010) 1–7.
[25] K. Uchino, S. Nomura, Ferroelectr. Lett. Sect. 44 (1982) 55.
[26] L.E. Cross, Ferroelectrics 151 (1994) 305.
[27] Z.-G. Ye, Key Eng. Mater. 81 (1998) 155–156.
[28] I.W. Chen, J. Phys. Chem. Solids 61 (2000) 197.
[29] A.A. Bokov, Z.-G. Ye, J. Mater. Sci. 41 (2006) 31.
[30] X. Long, Z.-G. Ye, Appl. Phys. Lett. 90 (2007) 112905.